Kumars Rouzbehi, Álvaro Luna, Joan Rocabert, Pedro Catalán, Pedro Rodríguez. (2018) Fuzzy gain scheduling based grid synchronization system responsive to the electrical network conditions. *ECCE 2018: IEEE Energy Conversion Congress and Exposition: Portland, OR, USA: Sept. 23-27, 2018* : IEEE, 2018. Pp. 3120-3125 Doi: 10.1109/ECCE.2018.8558318.

Kumars Rouzbehi, Álvaro Luna, Joan Rocabert, Pedro Catalán, Pedro Rodríguez. (2018) Fuzzy gain scheduling based grid synchronization system responsive to the electrical network conditions. *ECCE 2018: IEEE Energy Conversion Congress and Exposition: Portland, OR, USA: Sept. 23-27, 2018* : IEEE, 2018. Pp. 3120-3125 Doi: 10.1109/ECCE.2018.8558318.

Fuzzy Gain Scheduling based Grid Synchronization System Responsive to the Electrical Network Conditions

Kumars Rouzbehi
Department of Engineering
University of Loyola Andalucía
Sevilla, Spain
qrouzbehi@uloyola.es

Alvaro Luna
Department of Electrical Engineering
Universitat Poliècnica de Catalunya
Barcelona, Spain
luna@ee.upc.edu

Joan Rocabert
Department of Electrical Engineering
Universitat Poliècnica de Catalunya
Barcelona, Spain
rocabert@ee.upc.edu

Pedro Catalán
Wind Energy - Energy Division
Ingeteam Power Technology
Bilbao, Spain
pedro.catalan@ingeteam.com

Pedro Rodríguez
Department of Engineering
University of Loyola Andalucía
Sevilla, Spain
prodriguez@uloyola.es

***Abstract*—In power conversion applications grid synchronization systems should face very different network operating conditions such as: generic grid connection, faulty or distorted scenarios or islanded conditions among others. However, all the existing synchronization systems have issues operating in all these scenarios if the control tuning parameters cannot be adapted to the grid conditions. This paper proposes a Fuzzy Gain Scheduling PLL (FGS-PLL) to be used for grid synchronization, which has a robust performance in case of severe voltage sag, where there is even a null value of voltage, and phase jump conditions. Moreover, the proposed method employs a fuzzy gain scheduling technique to adjust the proportional and integral gains of the proposed PLL during amplitude, phase and frequency variations in the grid voltage waveform to build a flexible PLL in case of severe grid conditions. This PLL structure permits to adjust the performance in different conditions as well as to provide a voltage reference, even in case of 100% voltage sag**

Keywords*—*component, formatting, style, styling, insert (key words)

I. Introduction

In order to synchronize with the grid voltage, Synchronous Reference Frame - Phase Locked Loops (SRF-PLLs) are commonly implemented in the control algorithm of grid-connected power converters. A typical PLL comprises a Phase Detector (PD), a Low Pass Filter (LPF) and a Voltage Controlled Oscillator (VCO) [1]. Nevertheless, the performance of such PLLs also depends on the grid conditions [2]. For instance, if the voltage goes below a certain threshold the PLL is unable to make a good synchronization if the tuning parameters are not changed. This is for instance the case of power converters when they are requested to provide Low Voltage Ride Through, even when there is a voltage sag that forces the voltage to zero [3]-[5]. In this paper, in order to improve the SRF-PPL's performance during severe contingencies in the grid voltage, a Fuzzy Gain-Scheduling (FGS) strategy is developed for the SRF- PLL structure.

This work has been supported by the Spanish Ministry of Economy and Competitiveness under the projects ENE2016-79493-R and ENE2017-88889-C2-1-R.

The proposed FGS strategy slows down the SRF-PLL response speed when the grid voltage amplitude descends. In this way, the fluctuations of the PLL response to voltage variations will significantly reduce and the performance of PLL will considerably improve [6]-[7]. Moreover a specific limitation that permits to frozen the output and keeps its performance as an oscillator is implemented.

In this work, to implement the FGS strategy, a fuzzy inference system (FIS) is developed and validated by the laboratory test system. The FIS is established based on a set of rules, which determine PLL speed. Moreover, in order to provide a fast decision by the FIS, the amplitude of the grid voltage is estimated using a fast estimation algorithm, known as Mann-Morrison technique. In case of severe voltage dip (for instance below than 0.2 pu) the freeze mode is introduced to freeze the tracking action of the PLL.

II. Fuzzy Gain-Scheduling Strategy

The overall control structure of the PLL with FGS is illustrated in Fig. 1. According to this structure, the three-phase voltages, i.e., v_{sa}, v_{sb} and v_{sc}, are used by a fast amplitude estimator (FAE), developed Based on the Mann-Morrison technique, to estimate amplitude of the grid's voltage, (or average of estimated voltage of three phases, AEV).

The general structure of the proposed FGS strategy is shown in Fig. 1. It's seen that the FGS for the integral gain, i.e. FGSi, only uses average estimate voltage of three phases (AEV) while the FGS for the proportional gain (FGSp) employs the AEV as well as the error of v_{sq}. The parameters of the PI controller are modified based on the FGSi and FGSp, as stated below, where, α_i and α_p are the output of the FGSi and FGSp, respectively, and k_p^* and k_i^* are the modified proportional and integral gains" of the PI controller, respectively.

$$k_p^* = \alpha_p \times k_p \tag{1}$$

$$k_i^* = \alpha_i \times k_i \tag{2}$$

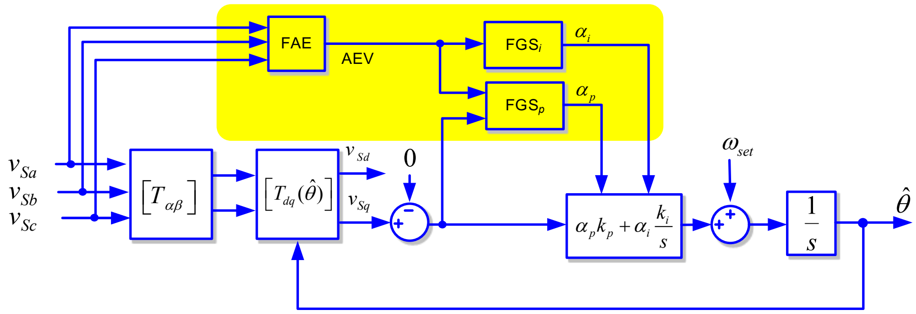

Fig. 1. Structure of the PLL with fuzzy gain scheduling.

The FGSp block includes two inputs (AEV and v_{sq}) and one output (α_p). The rule table for the FGS block is presented in Table 1.

TABLE I. TABLE OF RULES

AEV / v_{sq}	Z	PS	PM	PB
S	Z	PS	PM	PB
B	PS	PM	PB	PB

In this table, "Z", "PS", "PM", and "PB" are the membership functions associated with the input AEV and stand for zero, positive small, positive medium, and positive big, respectively.
On the other hand, "S" and "B" are the membership functions of the input v_{sq} and stand for small and big, respectively. The input and output membership functions are shown in Figs. 2, respectively.

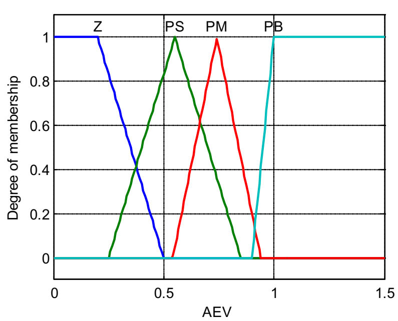

(a)

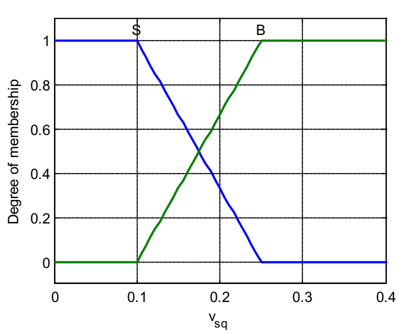

(b)

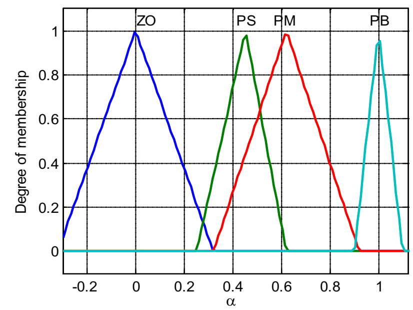

(c)

Fig. 2 . (a) Membership functions of input AEV for FGS$_p$ (b) Membership functions of input v_{sq} for FGS$_p$ (c) Output membership functions of FGS$_p$

Moreover, the output variable α_p includes the following membership functions: "ZO", "PS", "PM", and "PB". These membership functions are shown in Figs. 2a – c . Moreover, the fuzzy surface of the FGSp is illustrated in Fig. 3.

In a FIS, or fuzzy systems in general, the dynamic behavior of that system is characterized by a set of fuzzy rules. These rules are based on the knowledge and experience of a human expert within that domain. The fuzzy rules are a major part of form the knowledge base of a fuzzy rule-based reasoning system.

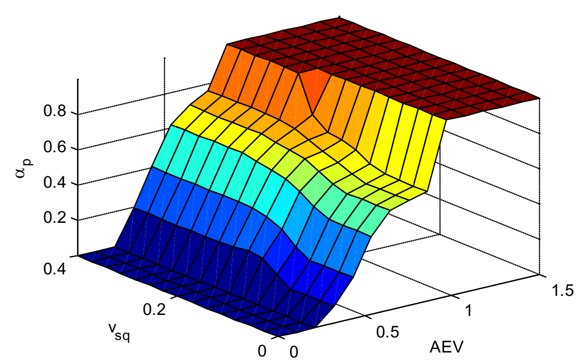

Fig. 3. Fuzzy surface of FGS$_p$

However, in addition to the fuzzy rules, a FIS includes three other components, each performing a specific task in the reasoning process, i.e., fuzzification, inferencing, and defuzzification.

The fuzzification process is concerned with finding a fuzzy representation of non-fuzzy input value, here the AEV. This is achieved through application of the membership functions associated with each fuzzy set in the rule input space. That is, input values (AEV) are assigned membership values to fuzzy sets. For instance, for AEV=0.40, the fuzzification of the input produces the following membership degrees: 0.6 for Z, 0.21 for PS and 0 for PM and PB, as shown in Fig. 3(d).

In the inference stage, the fuzzified input (as received from the fuzzification process) is mapped to the rule base; a fuzzified output is produced for each rule. This procedure is shown in Fig. 4(a).

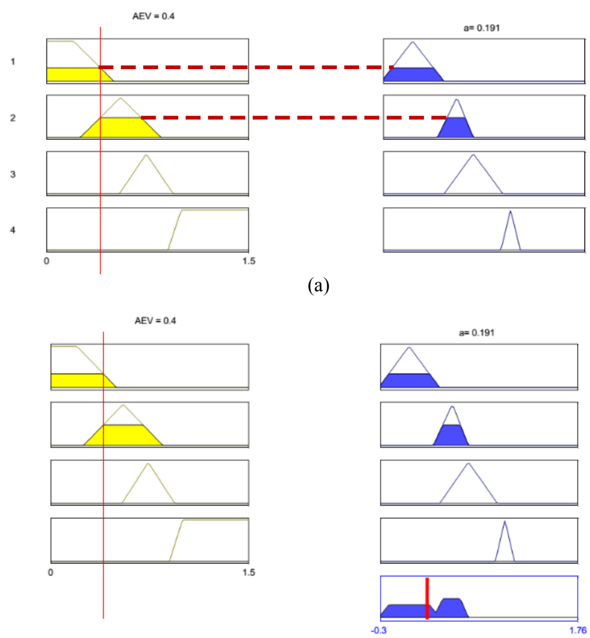

Fig. 4 (a) Inference result for input (b) Defuzzification process for input

In the defuzzification process, the output of the fuzzy rules is converted into a scalar, or non-fuzzy value. This is carried out by finding the center of gravity of the composite area, constructed by clipping and aggregating the output fuzzy membership function, as shown in Fig. 2(c).

III. Fast Amplitude Estimator

One of the objectives of the proposed synchronization system is to retune the PLL based on the grid conditions. The voltage magnitude influence in speed of the grid synchronization loop. If we can retune the controller based on the amplitude of the signal we can adjust the dynamics in different scenarios. Due to this having a fast, either not accurate, amplitude estimator is an advantage.

Mann-Morrison three-point estimation algorithm is a fast technique for amplitude estimation of sinusoidal signals. It is based on approximating the derivative of the signal based on the three available samples, V^-, V^0, V^+.

$$V^0 = V_m \sin(\omega t)\big|_{t=t_0} \tag{3}$$

$$\frac{dv}{dt}\bigg|_{t=t_0} = V_m \omega \cos(\omega t)\big|_{t=t_0} \tag{4}$$

By applying the following approximation of signal derivative:

$$\frac{dv}{dt}\bigg|_{t=t_0} \approx \frac{V^+ - V^-}{2\Delta t} \tag{5}$$

and combining (3) and (5), the following is obtained,

$$\left(\omega V^0\right)^2 + \left(\frac{V^+ - V^-}{2\Delta t}\right)^2 = V_m^2 \omega^2 \tag{6}$$

Solving (6) for V_m results in

$$V_m = \frac{1}{\omega}\sqrt{\left(\omega V^0\right)^2 + \left(\frac{V^+ - V^-}{2\Delta t}\right)^2} \tag{7}$$

By applying (7), a fast estimation for V_m is provided by use of only three signal samples.

IV. Validation Results

In this validation stage the grid voltage measurements are extracted from real data recorded in a wind turbine test bench. The performance of the FGS-based PLL are compared with the ones obtained with a conventional PLL without FGS.

A. *Study Case of a Severe Voltage Sag*

The waveforms of a voltage sag recorded in the test are shown in Fig. 5(a). In this case two consecutive faults appear; the first sag happens at t = 0.3 sec, while the second (which is more severe) occurs at t = 1 sec.

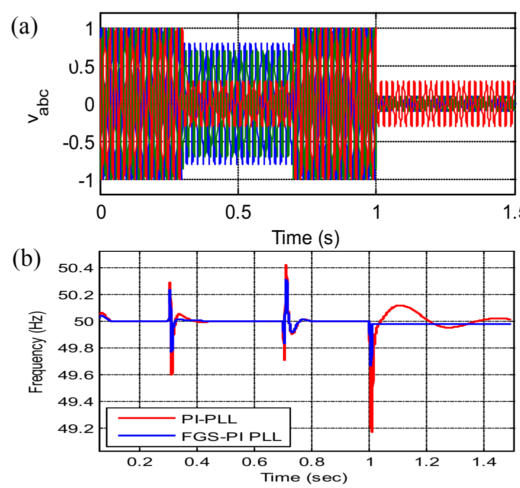

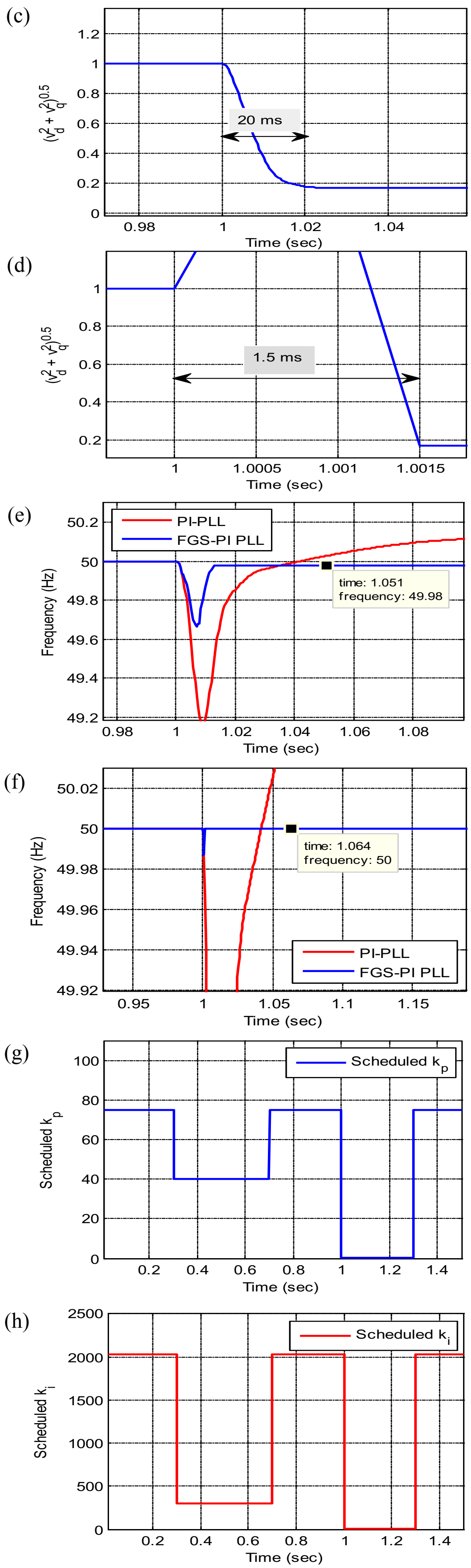

Fig. 5 **(a)** Voltage waveform in first case **(b)** Frequency estimation by PI-PLL and FGS-PI-PLL **(c)** Delay in normal estimation of voltage amplitude **(d)** Performance of fast amplitude estimator **(e)** Frequency error in freeze mode due to delay in voltage amplitude estimation **(f)** Exact frequency estimation in freeze mode due to the performance of fast amplitude estimator **(g)** Variation of kp during voltage evolutions **(h)** Variation of ki during voltage evolutions

The estimation of the positive sequence amplitude is shown in Fig. 5(c) focused on the second sag when the FGS-PLL is used, while the same estimation made by a conventional PLL is depicted in Fig. 5(d). Likewise, the frequency estimation in both cases are plotted in Fig. 5(b).and a zoom view of the estimation around the sag point are shown in Fig. 5(e) and Fig. 5(f).

As it can be concluded from the results the amplitude and the frequency are better detected with the FGS.PLL, as this synchronization system adapts the gain of the PI in the PLL as a function of the magnitude. The values of the PI parameters and how they change are shown in Fig. 5(g) and Fig. 5(h).

It is worth to remark that at $t = 1$, the voltages of all phases fall severely, leading to activation of PLL's freeze mode. In this circumstance, the simple PLL (without FGS) shows an oscillatory response. However, due to the delay in voltage amplitude detection, the PLL cannot lock in the actual value of frequency in freeze mode.

B. Study Case of Unbalanced Voltage Sags C and D

The voltage sag that give rise to the Type C and Type D curves is the most common one that can be found in faulty scenarios. This is due to the fact that almost 95% of voltage dips are due to the impact of lightnings that connect one phase to the ground. The transformation of this fault caused by the interconnection of transformer windings give rise to a type C or D sag.

The results obtained in this case are depicted in Fig. 6, where it can be seen the better performance of the proposed FGS-PI-PLL.

In Fig. 6(b) the estimation of the frequency in case of Sag C when using FGS-PLL and a conventional PLL is shown. The same comparison is made in Fig. 6(d) when the performance in case of Sag D is analyzed. In both case the adaptation of parameters that the FGS-PLL provides permits offering a better performance with lower overshoot in the transient.

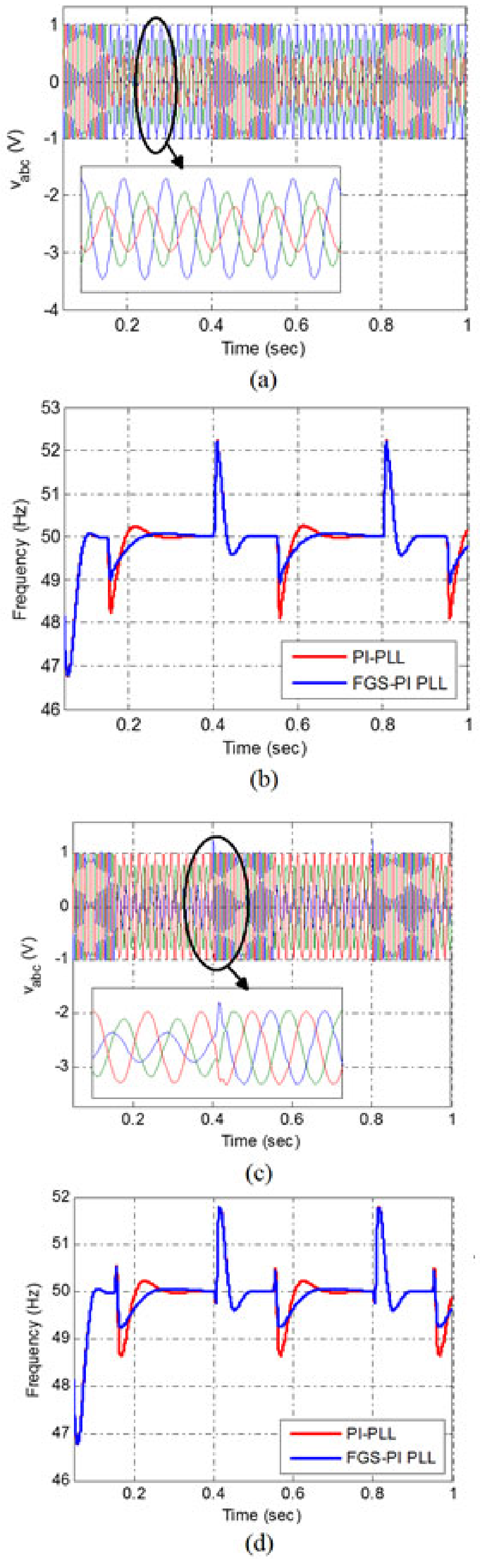

Fig. 6 *Test results on signals 3 and 4* **(a)** *Voltage waveform for Sag C* **(b)** *Frequency estimation for Sag C* **(c)** *Voltage waveform for Sag D* **(d)** *Frequency estimation for Sag D*

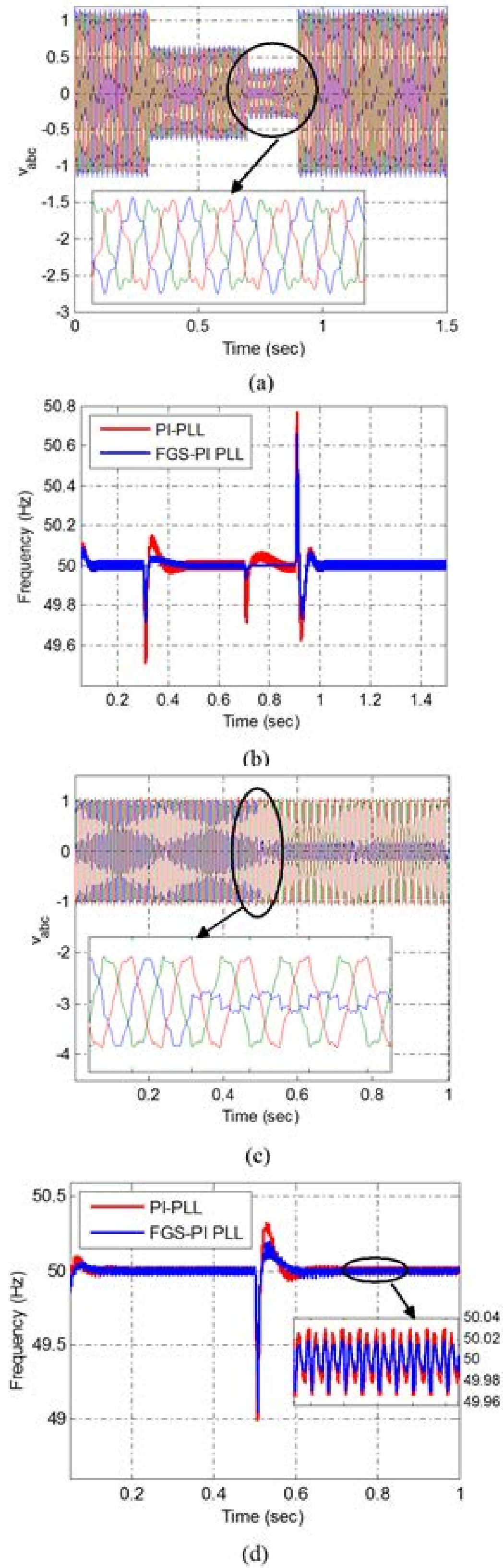

Fig. 7 *Voltage waveform contaminated with fifth harmonic (b) Frequency estimation of the harmonic voltage waveform (c) Severe voltage dip on phase A at t = 0.5 sec with THD = 8% (d) Frequency estimation of the harmonic voltage waveform with severe voltage dip on phase A*

C. *Study Case of Harmonic Distortion*

In order to validate that the response of the proposed system is not affected by harmonic signals a last test have been considered taking into account the harmonic content considered by the EN50160.

In an initial test effect of the harmonics on PLL's performance, considering 5% of fifth harmonics is added to the signal, as shown in Fig. 7(a). The results for this case are illustrated in Fig. 7(b). Clearly, the proposed FGS-PLL has superior performance of the PI-PLL.

Moreover, results for a severe unbalanced three-phase voltage with a total harmonic distortion of 8% (i.e. 6% of 5^{th} harmonic, 5% of 7^{th} harmonic, 3.5% percent of 11^{th} harmonic and 3% of 13^{th} harmonic), as shown in Fig. 7(c) is used. The performances of the FGS-PLL and PI-PLL are shown in Fig. 7(d). Again, the proposed approach exhibits better performance.

V. Conclusions

This paper proposed a fuzzy gain scheduled PLL to address the issues related to sever voltage sag and phase jump and frequency conditions. The proposed approach takes advantage of a fuzzy gain scheduling system to adjust the proportional and integral gains of the PLL during amplitude, phase and frequency variations in the voltage waveform. Moreover, Mann-Morrison three-point estimation algorithm was used to provide quick and fairly accurate estimates of the three-phase voltage amplitude. Results of various simulation scenarios as well as laboratory experimentals of different types of voltage waveforms demonstrated the reliable performance of the proposed approach under a variety of severe voltage waveform conditions.

Acknowledgment

This work has been supported by the Spanish Ministry of Economy and Competitiveness under the projects ENE2016-79493-R and ENE2017-88889-C2-1-R. Any opinions, findings and conclusions or recommendations expressed in this material are those of the authors and do not necessarily reflect those of the host institutions or funderse.

References

[1] Liccardo, F., P. Marino, and G. Raimondo, *Robust and fast three-phase PLL tracking system.* Industrial Electronics, IEEE Transactions on, 2011. **58**(1): p. 221-231.

[2] Escobar, G., et al., *Fixed-reference-frame phase-locked loop for grid synchronization under unbalanced operation.* Industrial Electronics, IEEE Transactions on, 2011. **58**(5): p. 1943-1951.

[3] Silva, C.H.d., et al., A digital PLL scheme for three-phase system using modified synchronous reference frame. Industrial Electronics, IEEE Transactions on, 2010. 57(11): p. 3814-3821.

[4] Rodríguez, P., et al., A stationary reference frame grid synchronization system for three-phase grid-connected power converters under adverse grid conditions. Power Electronics, IEEE Transactions on, 2012. **27**(1): p. 99-112.

[5] Thacker, T., et al., *Phase-locked loop noise reduction via phase detector implementation for single-phase systems.* Industrial Electronics, IEEE Transactions on, 2011. **58**(6): p. 2482-2490.

[6] González-Espín, F., E. Figueres, and G. Garcerá, *An adaptive synchronous-reference-frame phase-locked loop for power quality improvement in a polluted utility grid.* Industrial Electronics, IEEE Transactions on, 2012. **59**(6): p. 2718-2731.

[7] Dong, D., et al., Analysis of Phase-Locked Loop Low-Frequency Stability in Three-Phase Grid-Connected Power Converters Considering Impedance Interactions. Industrial Electronics, IEEE Transactions on, 2015. **62**(1): p. 310-321.